JACS
JOURNAL OF THE AMERICAN CHEMICAL SOCIETY

Article

pubs.acs.org/JACS

Controlled Formation of Heteroleptic $[Pd_2(L_a)_2(L_b)_2]^{4+}$ Cages

Dan Preston, Jonathan E. Barnsley, Keith C. Gordon, and James D. Crowley*

Department of Chemistry, University of Otago, P.O. Box 56, Dunedin 9054, New Zealand

Supporting Information

ABSTRACT: Metallosupramolecular architectures are beginning to be exploited for a range of applications including drug delivery, catalysis, molecular recognition, and sensing. For the most part these achievements have been made with high-symmetry metallosupramolecular architectures composed of just one type of ligand and metal ion. Recently, considerable efforts have been made to generate metallosupramolecular architectures that are made up of multiple different ligands and/or metals ions in order to obtain more complex systems with new properties. Herein we show that the addition of an electron-rich 2-amino-substituted tripyridyl ligand, 2,6-bis(pyridin-3-ylethynyl)pyridine (**2A-tripy**), to a solution of the $[Pd_2(\mathbf{tripy})_4]^{4+}$ cage resulted in the clean generation of a heteroleptic $[Pd_2(\mathbf{tripy})_2(\mathbf{2A\text{-}tripy})_2]^{4+}$ architecture. The formation of the mixed-ligand cage $[Pd_2(\mathbf{tripy})_2(\mathbf{2A\text{-}tripy})_2]^{4+}$ was confirmed using ^{1}H NMR spectroscopy, diffusion-ordered spectroscopy, and rotating-frame nuclear Overhauser effect spectroscopy and high-resolution electrospray ionization mass spectrometry. Density functional theory calculations suggested the *cis* isomer was more stable that the *trans* isomer. Additionally, the calculations indicated that the heteroleptic palladium(II) cages are kinetically metastable intermediates rather than the thermodynamic product of the reaction. Competition experiments supported that finding and showed the cages are long-lived in solution at room temperature. Finally, it was shown that the addition of **2A-tripy** to a range of preformed $[Pd_2(\mathbf{L}_{\mathbf{tripy}})_4]^{4+}$ cages cleanly generated the mixed-ligand systems. Three other systems displaying different *exo* and *endo* functionalities within the cage assembly were generated, suggesting that this method could be applied to synthesize a range of highly functionalized heteroleptic *cis*-$[Pd_2(\mathbf{L}_a)_2(\mathbf{L}_b)_2]^{4+}$ cages.

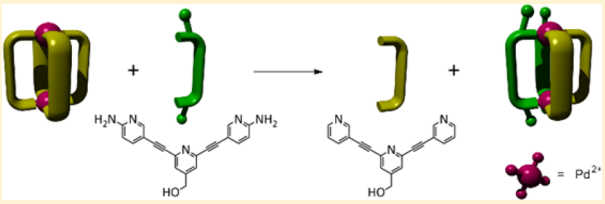

INTRODUCTION

The potential uses for metallosupramolecular architectures, self-assembled coordination complexes of well-defined two- and three-dimensional geometries,[1] continue to grow. The molecular recognition properties of these systems have been exploited to sequester reactive species[2] and environmental pollutants,[3] while other architectures have been used as molecular reaction flasks,[4] catalysts,[5] and drug delivery agents.[6] Furthermore, these metallosupramolecular architectures have been shown to display interesting biological,[7] photophysical,[8] and redox[9] properties.

For the most part these achievements have been made with high-symmetry metallosupramolecular architectures composed of just one type of ligand and metal ion. Recently efforts have been made to generate more-complex metallosupramolecular architectures[10] that are made up of multiple ligands and/or metal ions.[11] It is reasoned that increasing the complexity of the metallosupramolecular architecture will lead to new chemistry/functionality.[12] However, methods that allow the *controlled* generation of heteroleptic polyfunctionalized metallosupramolecular architectures remain rare.

Square planar palladium(II) ions have been extensively used to generate metallosupramolecular architectures.[13] This is at least in part due to the favorable combination of kinetic lability but thermodynamic stability in the Pd(II)−ligand interaction, which generally enables self-assembly to proceed in high yields. Both "naked"[14] and *cis*-protected[15] palladium complexes have been used to generate two- and three-dimensional architectures. Several strategies exist for the generation of lower symmetry heteroleptic metallosupramolecular architectures from *cis*-protected palladium complexes.[16] However, methods for the synthesis of heteroleptic architectures from "naked" palladium complexes are not as well developed.[17] Several groups have examined the outcome of mixing "naked" palladium(II) ions with two different di- or tripyridyl ligands ($\mathbf{L}_a$ and $\mathbf{L}_b$). There are three potential outcomes: (1) narcissistic self-sorting, resulting in the clean formation of two different homoleptic cages (e.g., $[Pd_2(\mathbf{L}_a)_4]^{4+}$ and $[Pd_2(\mathbf{L}_b)_4]^{4+}$, Figure 1a); (2) promiscuous ligand dispersal, resulting in the formation of a (roughly) statistical mixture of homo- and heteroleptic cages (Figure 1b); and (3) controlled social self-sorting into uniform heteroleptic assemblies (e.g., $[Pd_2(\mathbf{L}_a)_2(\mathbf{L}_b)_2]^{4+}$, Figure 1c). For the most part, mixing palladium(II) ions with two different ligands ($\mathbf{L}_a$ and $\mathbf{L}_b$) has resulted in the formation of statistical or amplified mixtures of cage complexes without selectivity (Figure 1b).[18]

Hooley and co-workers have examined the formation of a series of $[Pd_2(\mathbf{L})_4]^{4+}$ architectures using "banana-shaped" endohedrally substituted dipyridyl ligands.[19] When unsubstituted ($\mathbf{L}_a$) and endohedrally substituted ($\mathbf{L}_b$) ligands with a small substituent (R = NH_2) were mixed with palladium(II) ions, a statistical mixture of homo- and heteroleptic cages was observed to form. Self-sorting behavior was observed when the

Received: June 1, 2016
Published: July 27, 2016

DOI: 10.1021/jacs.6b05629
J. Am. Chem. Soc. 2016, 138, 10578−10585

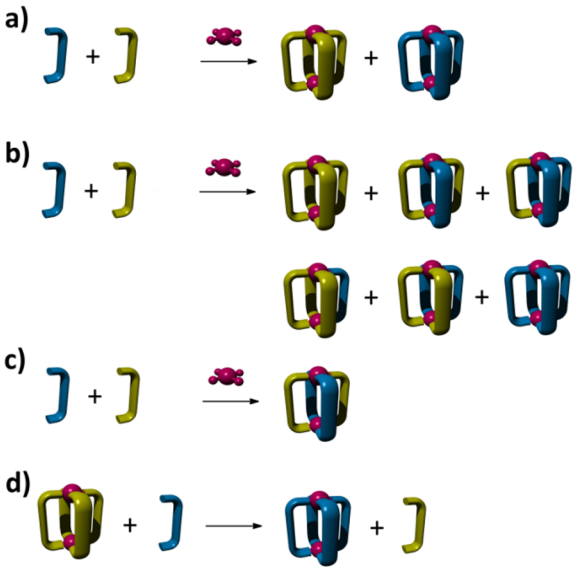

Figure 1. Generic cartoon representations showing the potential outcomes of mixing two different "banana-shaped" ligands ($\mathbf{L_a}$ (blue) and $\mathbf{L_b}$ (yellow)) with "naked" Pd(II) ions, generating $[Pd_2(\mathbf{L})_4]^{4+}$ metallosupramolecular assemblies: (a) narcissistic self-sorting from varied ligands, (b) promiscuous ligand dispersal into statistical or amplified mixtures, (c) controlled social self-sorting into uniform heteroleptic assemblies, and (d) ligand displacement to give a narcissistic homoleptic complex.

experiment was repeated using a larger endohedral substituent (R = NHC(O)CF_3) on $\mathbf{L_b}$. A mixture of the homoleptic unsubstituted $[Pd_2(\mathbf{L_a})_4]^{4+}$ and heteroleptic $[Pd_2(\mathbf{L_a})_3(\mathbf{L_b})]^{4+}$ cages formed, and this was controlled by the steric requirements of the endohedrally substituted ligand ($\mathbf{L_b}$).[19] However, as this approach exploited the steric bulk of the *endo* substituent to fill the cage cavity and drive the formation of the mixed-ligand species, the resulting heteroleptic cages cannot be used for binding other guest molecules.

Yoshizawa and co-workers have shown that similar "banana-shaped" dipyridyl ligands will form $[Pd_2(\mathbf{L})_4]^{4+}$ architectures.[20] When they mixed cages containing long ($\mathbf{L_a}$) and short ($\mathbf{L_b}$) ligands, a statistical mixture of homo- and heteroleptic cages formed. Addition of a guest (C_{60}) to this statistical mixture templated the formation of the heteroleptic *cis*-$[(C_{60})\subset Pd_2(\mathbf{L_a})_2(\mathbf{L_b})_2]^{4+}$ cage–guest adduct.[18a]

Narcissistic self-sorting of homoleptic cage complexes has been observed. Addition of a stronger ligand to a preformed Pd(II) cage causes the displacement of the weaker ligands, generating a new homoleptic cage composed of the stronger ligand (Figure 1d).[18b,21] Mukherjee and co-workers reported an example of this behavior, where addition of a dipyridyl ligand to a pyrimidine-based $[Pd_{24}(\mathbf{L_a})_{24}]^{48+}$ assembly resulted in the complete conversion into a new pyridine-based $[Pd_{12}(\mathbf{L_b})_{24}]^{24+}$ nanoball.[21] Similar results have been obtained by Hardie and co-workers with a $[Pd_6(\mathbf{L_a})_8]^{12+}$ system.[18b] Clever and co-workers have found that mixing a long ($\mathbf{L_a}$) and a short ($\mathbf{L_b}$) "banana-shaped" dipyridyl ligand with Pd(II) ions leads to the narcissistic self-assembly of a interlocked double-cage $[Pd_4(\mathbf{L_a})_8]^{8+}$ and a small monomeric $[Pd_2(\mathbf{L_b})_4]^{4+}$ cage, regardless of the order of mixing and Pd(II) addition.[22]

More difficult to achieve is the controlled formation of uniform heteroleptic assemblies. This could occur through two different processes, either by combining two different ligands and a metal (Figure 1c) or through ligand displacement from a preformed cage. Fujita and co-workers have generated a uniform heteroleptic $[Pd_{12}(\mathbf{L_a})_{12}(\mathbf{L_b})_{12}]^{24+}$ cantellated tetrahedron through size-based controlled social sorting.[23] Combining long ($\mathbf{L_a}$) and short ($\mathbf{L_b}$) dipyridyl ligands with Pd(II) ions in a 1:1:1 ratio led to the clean formation of the heteroleptic $[Pd_{12}(\mathbf{L_a})_{12}(\mathbf{L_b})_{12}]^{24+}$ architecture. The heteroleptic formulation was confirmed using CSI-MS and X-ray crystallography. Conversely, addition of either $\mathbf{L_a}$ or $\mathbf{L_b}$ to palladium(II) ions in a 1:2 ratio generated homoleptic $[Pd_{12}\mathbf{L_{24}}]^{24+}$ architectures of a cuboctahedral geometry.[23]

Very recently, Mukherjee and co-workers have shown that mixing $Pd(NO_3)_2$, a "clip" like 3,3-(1*H*-1,2,4-triazole-3,5-diyl)dipyridine ($\mathbf{L_a}$) and a linear ditopic 1,4-di(4-pyridylureido)benzene ($\mathbf{L_b}$) in a 1:1:1 ratio in d_6-DMSO solution results in the formation of a heteroleptic trigonal prismatic $[Pd_6(\mathbf{L_a})_6(\mathbf{L_b})_6]^{12+}$ architecture.[24] However, the authors provide no rationale for the selective formation of the heteroleptic prism over the homoleptic cage and polymers.

While both of the above approaches cleanly generate uniform heteroleptic palladium(II)-based assemblies, it is not clear that either provides a rapid, reliable, general strategy that could be applied for the generation of other palladium(II)-containing heteroleptic metallosupramolecular architectures.

As part of our interest in the molecular recognition properties of metallosupramolecular architectures,[25] we have previously reported the synthesis of a tripyridyl (**tripy**) $[Pd_2(\mathbf{L})_4]^{4+}$ cage[26] capable of binding cisplatin.[27] However, efforts to exploit these types of $[Pd_2(\mathbf{L})_4]^{4+}$ cages as metallosupramolecular drug delivery vectors were hampered by the instability of the system in the presence of common biological nucleophiles such as chloride (Cl^-),[27,28] histidine (his),[28b] and cysteine (cys).[28b] One obvious approach to increase the kinetic stability of these metallosupramolecular architectures against nucleophiles was to sterically and electronically tune the **tripy** ligand framework. As such, we generated two new, more electron-rich amino-substituted tripyridyl ligands (**2A-tripy** and **3A-tripy**) and their respective cages (Figure 2).[29] Addition of the amino groups to the 2- and 3-positions of the terminal ligating pyridyl units of the ligand framework increased the donor properties of the ligands and, in the case of **2A-tripy**, provided steric protection of the metal and interligand hydrogen-bonding interactions, which resulted in more kinetically robust cage architectures.[29]

Herein, we report an interesting discovery made during the course of carrying out competition experiments with these new electron-rich amino-substituted tripyridyl ligands (**2A-tripy** and **3A-tripy**) and the parent unsubstituted $[Pd_2(\mathbf{tripy})_4]^{4+}$ cage. As expected, addition of the **3A-tripy** ligand to the preformed $[Pd_2(\mathbf{tripy})_4]^{4+}$ cage led to complete displacement of **tripy** from the cage system and the clean formation of $[Pd_2(\mathbf{3A\text{-}tripy})_4]^{4+}$ architectures. More interestingly, we hypothesized that the steric bulk of **2A-tripy**, in conjunction with its higher donor strength and interligand hydrogen-bonding capability, might provide the opportunity for partial displacement. This is indeed the case, and we have uncovered a new approach to the generation of uniform heteroleptic palladium(II)-based assemblies. Addition of **2A-tripy** ligands to a solution of the preformed $[Pd_2(\mathbf{tripy})_4]^{4+}$ cage leads to the selective formation of the heteroleptic *cis*-$[Pd_2(\mathbf{2A\text{-}tripy})_2(\mathbf{tripy})_2]^{4+}$ architecture. The method proved general, and a small series of heteroleptic $[Pd_2(\mathbf{L_a})_2(\mathbf{L_b})_2]^{4+}$ cages with different *exo* functionalization or cavity environments were generated. It is expected that this

DOI: 10.1021/jacs.6b05629
J. Am. Chem. Soc. 2016, 138, 10578–10585

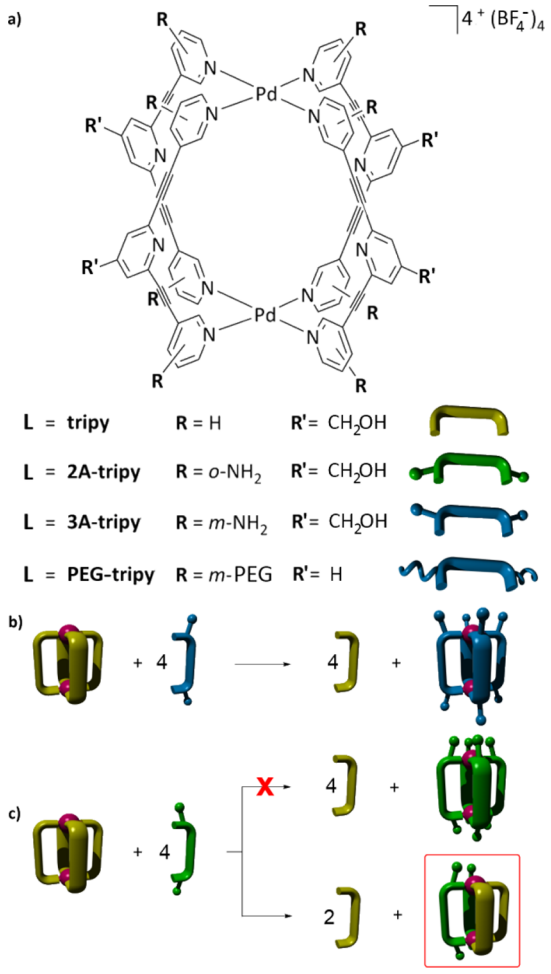

Figure 2. (a) Previously synthesized $[Pd_2(L_{tripy})_4]^{4+}$ cages from the tripyridyl ligands (**tripy**, **2A-tripy**, **3A-tripy**, and**PEG-tripy**). Generic cartoon representations showing the exchange reactions between (b) $[Pd_2(\textbf{tripy})_4]^{4+}$ and **3A-tripy** with complete displacement, and (c) $[Pd_2(\textbf{tripy})_4]^{4+}$ and **2A-tripy**, which did not lead to complete displacement (top) but instead gave partial displacement (bottom). Note, for simplicity, excess free **2A-tripy** is not shown in products from partial displacement.

general approach to the formation of palladium(II)-containing heteroleptic architectures should enable the development of more sophisticated polyfunctionalized metallosupramolecular architectures.

RESULTS AND DISCUSSION

The electronically and sterically tuned tripyridyl ligands (**tripy**,[29] **2A-tripy**,[29] **3A-tripy**,[29] and **PEG-tripy**,[28a] where PEG = 2-(2-methoxyethoxy)ethoxy) and the corresponding $[Pd_2(L_{tripy})_4](BF_4)_4$ cages ($[Pd_2(\textbf{PEG-tripy})_4]^{4+}$,[28a] $[Pd_2(\textbf{tripy})_4]^{4+}$, $[Pd_2(\textbf{3A-tripy})_4]^{4+}$, and $[Pd_2(\textbf{2A-tripy})_4]^{4+}$)[29] were synthesized as previously reported (Figure 2a). Competition experiments[30] (Supporting Information, Figure S1.1) were then conducted by the addition of either the **2A-tripy** or **3A-tripy** ligand to a solution of the preformed $[Pd_2(\textbf{tripy})_4]^{4+}$ cage (Figure 2b,c). Titration of **3A-tripy** into a 298 K d_6-DMSO solution of $[Pd_2(\textbf{tripy})_4]^{4+}$ led to the complete conversion of the parent cage into $[Pd_2(\textbf{3A-tripy})_4]^{4+}$ and the liberation of four **tripy** ligands, as shown by ^{1}H NMR and electrospray ionization mass spectrometry (ESI-MS) experiments (Figure 2b and Supporting Information, Figures S1.2 and S1.3). The conversion was rapid and complete in less than 1 min (the time required to acquire a ^{1}H NMR spectrum of the mixture). These rapid kinetics are similar to those observed for the formation of the homoleptic cages $[Pd_2(\textbf{tripy})_4]^{4+}$ and $[Pd_2(\textbf{3A-tripy})_4]^{4+}$.[29]

Simply mixing the ligands (**tripy**, **3A-tripy**) and $[Pd(CH_3CN)_4](BF_4)_2$ in a 2:2:2 ratio generated a statistical mixture of heteroleptic cages, as evidenced by ^{1}H NMR and ESI-MS (Supporting Information, Figures S1.2j and S1.4). Similarly, when the two isolated cages $[Pd_2(\textbf{tripy})_4]^{4+}$ and $[Pd_2(\textbf{3A-tripy})_4]^{4+}$ were recombined in d_6-DMSO, over time they slowly scrambled, giving what appeared to be a statistical mixture of heteroleptic cages (Supporting Information, Figure S1.2k).

Intriguingly, a titration of preformed $[Pd_2(\textbf{tripy})_4]^{4+}$ with the **2A-tripy** ligand did not proceed in the same fashion as observed with the **3A-tripy** (Figures 2 and 3). Upon addition of

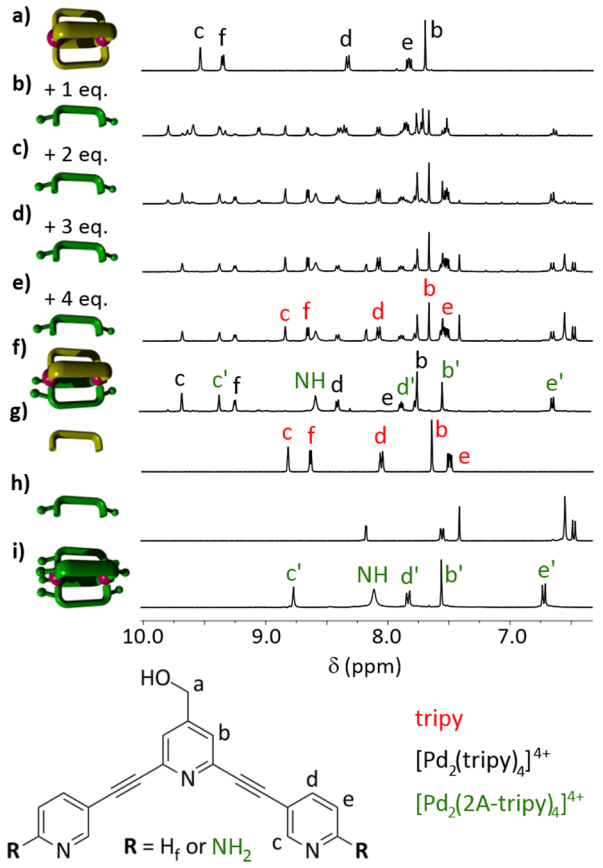

Figure 3. Partial ^{1}H NMR spectra (298 K, 400 MHz, d_6-DMSO) of (a) $[Pd_2(\textbf{tripy})_4]^{4+}$, (b) $[Pd_2(\textbf{tripy})_4]^{4+}$ + 1 equiv of **2A-tripy**, (c) $[Pd_2(\textbf{tripy})_4]^{4+}$ + 2 equiv of **2A-tripy**, (d) $[Pd_2(\textbf{tripy})_4]^{4+}$ + 3 equiv of **2A-tripy**, (e) $[Pd_2(\textbf{tripy})_4]^{4+}$ + 4 equiv of **2A-tripy**, (f) **tripy**, (g) **2A-tripy**, and (h) $[Pd_2(\textbf{2A-tripy})_4](BF_4)_4$.

different equivalencies (1−4 equiv) of the more electron-rich **2A-tripy** ligand to $[Pd_2(\textbf{tripy})_4]^{4+}$ in d_6-DMSO at 298 K (Figure 3b−e), the formation of several new assemblies was evident. The ligand-exchange processes were much slower than with **3A-tripy** and took 24 h to reach equilibrium. After 1 or 2 equiv of **2A-tripy** was added to the $[Pd_2(\textbf{tripy})_4]^{4+}$ cage, a variety of species could be seen, including the free ligands, $[Pd_2(\textbf{tripy})_4]^{4+}$, and other downfield-shifted peaks consistent with the formation of new "cage" complexes. Addition of further **2A-tripy** ligand (3 or 4 equiv) to the mixture generated

DOI: 10.1021/jacs.6b05629
J. Am. Chem. Soc. 2016, 138, 10578−10585

clean, sharp ^{1}H NMR spectra, showing only three species: the free ligands **tripy** and **2A-tripy**, and a third palladium(II)-containing species (Figure 3d,e) that was not the initial $[Pd_2(\mathbf{tripy})_4]^{4+}$ or the $[Pd_2(\mathbf{2A\text{-}tripy})_4]^{4+}$ cage (Figure 3a,h). The new species contains proton resonances for both **tripy** and **2A-tripy** in a 1:1 ratio. A diffusion-ordered spectroscopy (DOSY) NMR spectrum of the mixture shows that the proton resonances of both the **tripy** and **2A-tripy** components display the same diffusion coefficient (D = 1.01 × 10^{-10} m^{-2} s^{-1}, Supporting Information, Figure S1.5 and Table S1.1), indicating that they are part of the same molecule and are diffusing at a rate consistent with that expected for a $[Pd_2(L_{tripy})_4]^{4+}$ cage.[27−29]

Furthermore, the 2D rotating-frame nuclear Overhauser effect spectroscopy (ROESY) ^{1}H NMR spectrum (Figure 4)

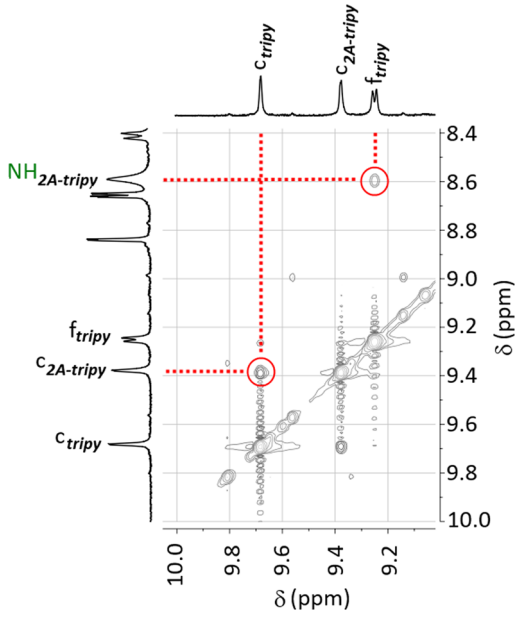

Figure 4. Partial 2D ROESY ^{1}H NMR spectrum (298 K, 500 MHz, d_6-DMSO, mixing time = 400 ms) of the reaction mixture obtained from the combination of $[Pd_2(\mathbf{tripy})_4](BF_4)_4$ with 4 equiv of **2A-tripy**.

showed a through-space coupling between the amino protons (NH_2) of **2A-tripy** and the exohedral proton *ortho* to the coordinating nitrogen of **tripy** (H_f). Likewise, a ROE cross-peak was observable between the *ortho* endohedral protons of both ligands (H_c of both **tripy** and **2A-tripy**). Mass spectral analysis of the solution only revealed a single peak consistent with a palladium(II)-containing species, at m/z = 379.5472, corresponding to $[Pd_2(\mathbf{tripy})_2(\mathbf{2A\text{-}tripy})_2]^{4+}$ ion (calcd m/z = 379.5681) (Supporting Information, Figure S1.6). Thus, addition of the **2A-tripy** ligand to the $[Pd_2(\mathbf{tripy})_4]^{4+}$ system resulted in the clean formation of a uniform heteroleptic $[Pd_2(\mathbf{tripy})_2(\mathbf{2A\text{-}tripy})_2]^{4+}$ cage assembly. HPLC analysis (Supporting Information, HPLC analysis 1.2.1, Figure S1.7) was also consistent with the ^{1}H NMR data. Analysis of a mixture of $[Pd_2(\mathbf{tripy})_4]^{4+}$ and 4 equiv of **2A-tripy** displays only peaks due to the two free ligands and $[Pd_2(\mathbf{tripy})_2(\mathbf{2A\text{-}tripy})_2]^{4+}$; no other species were observed.

The pure $[Pd_2(\mathbf{tripy})_2(\mathbf{2A\text{-}tripy})_2]^{4+}$ cage was then isolated by exploiting solubility differences between the two free ligands and the cage (Supporting Information, Synthesis 1.2.2 and Figures S1.8−S1.10). While the chemical composition of the new compound was now certain, it was unclear from the NMR spectra (due to high symmetry) whether the *cis* or *trans* isomer had formed.

To obtain information on the preferred isomer (*cis* or *trans*) and insight into the energetics of the reaction, density functional theory (DFT) calculations (gas phase, B3LYP with the LANL2DZ basis set for palladium atoms and the 6-31G(d) basis set for all other atoms, Supporting Information, 1.2.3 DFT calculations)[31] were carried out to determine the single-point energies for the ligands (**tripy**, **2A-tripy**, and **3A-tripy**), $[Pd(\mathbf{DMSO})_4]^{4+}$, and the cages $[Pd_2(\mathbf{tripy})_4]^{4+}$, $[Pd_2(\mathbf{2A\text{-}tripy})_4]^{4+}$, $[Pd_2(\mathbf{3A\text{-}tripy})_4]^{4+}$, and *cis*- and *trans*-$[Pd_2(\mathbf{tripy})_2(\mathbf{2A\text{-}tripy})_2]^{4+}$. The energy of formation (ΔE) for each cage system was then calculated using Hess's law (products minus reactants, equation S1, Supporting Information).

The calculations showed that the *cis* isomer is 19.3 kJ mol^{-1} lower in energy than $[Pd_2(\mathbf{tripy})_4]^{4+}$, whereas the *trans* isomer was found to be 7.9 kJ mol^{-1} higher in energy than the unsubstituted cage (Figure 5). These results suggest that the

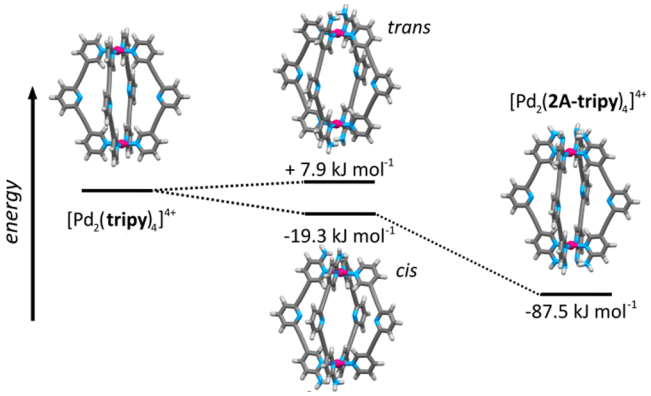

Figure 5. Energy diagram with calculated structures for $[Pd_2(\mathbf{tripy})_4]^{4+}$, *trans*-$[Pd_2(\mathbf{tripy})_2(\mathbf{2A\text{-}tripy})_2]^{4+}$, *cis*-$[Pd_2(\mathbf{tripy})_2(\mathbf{2A\text{-}tripy})_2]^{4+}$, and $[Pd_2(\mathbf{2A\text{-}tripy})_4]^{4+}$. Colors: magenta, palladium; gray, carbon; white, hydrogen; blue, nitrogen. For computational simplicity, the methylene alcohol units on the core pyridines were omitted. The *cis* isomer is 27.1 kJ mol^{-1} more stable than the *trans* isomer.

heteroleptic $[Pd_2(\mathbf{tripy})_2(\mathbf{2A\text{-}tripy})_2]^{4+}$ cage formed is the *cis* isomer (the *cis* isomer is 27.1 kJ mol^{-1} more stable than the *trans* isomer). The reason for the difference in energy between the two isomers can be attributed to a hydrogen-bonding interaction between the adjacent 2-amino units in the *cis* form (N---N 3.154 Å, N−H---N 2.136 Å, Supporting Information, Figure S1.12a) which is absent in the *trans* isomer (N---N 4.228 Å, N−H---N 3.505 Å, Supporting Information, Figure S1.12b).[32] The presence of this hydrogen-bonding interaction can be observed experimentally in the ^{1}H NMR spectrum of the $[Pd_2(\mathbf{tripy})_2(\mathbf{2A\text{-}tripy})_2]^{4+}$ cage. Upon formation of the homoleptic $[Pd_2(\mathbf{2A\text{-}tripy})_4]^{4+}$ cage, the resonance of the amino group protons undergoes a large downfield shift ($\Delta\delta$ = 1.56 ppm, 298 K, 500 MHz, d_6-DMSO), due to the interligand hydrogen-bonding.[29] The resonance of the 2-amino protons in the mixed cage undergoes a similar downfield shift of even larger magnitude ($\Delta\delta$ = 2.04 ppm), indicating that the 2-amino groups are still involved in substantial hydrogen-bonding interactions. We postulate that the larger shift observed for the *cis*-$[Pd_2(\mathbf{tripy})_2(\mathbf{2A\text{-}tripy})_2]^{4+}$ is caused by an additional hydrogen-bonding interaction between the 2-amino units of **2A-tripy** and the acidic α protons (H_f) on the adjacent **tripy**

DOI: 10.1021/jacs.6b05629
J. Am. Chem. Soc. 2016, 138, 10578−10585

ligands (Supporting Information, Figure S1.13). Comparison of the ^{1}H NMR spectra of the *cis*-$[Pd_2(\mathbf{tripy})_2(\mathbf{2A\text{-}tripy})_2]^{4+}$ and $[Pd_2(\mathbf{tripy})_4]^{4+}$ cages provides additional support for this postulate. The α protons (H_f) of *cis*-$[Pd_2(\mathbf{tripy})_2(\mathbf{2A\text{-}tripy})_2]^{4+}$ cage are found at δ = 9.24 ppm, while the corresponding signal in the $[Pd_2(\mathbf{tripy})_4]^{4+}$ cage was observed at δ = 9.05 ppm. The downfield shift ($\Delta\delta$ = 0.19 ppm) for the *cis*-$[Pd_2(\mathbf{tripy})_2(\mathbf{2A\text{-}tripy})_2]^{4+}$ cage is consistent with the presence of the additional hydrogen-bonding. Interestingly, the energy of the homoleptic 2-amino-substituted cage, $[Pd_2(\mathbf{2A\text{-}tripy})_4]^{4+}$, was found to be lower than that of the $[Pd_2(\mathbf{tripy})_4]^{4+}$ (−87.5 kJ mol^{-1}) and heteroleptic $[Pd_2(\mathbf{tripy})_2(\mathbf{2A\text{-}tripy})_2]^{4+}$ (−68.2 kJ mol^{-1} less than *cis*) cages (Figure 5). The calculated energies indicate that the $[Pd_2(\mathbf{2A\text{-}tripy})_4]^{4+}$ cage should be the thermodynamic product of the reaction of $[Pd_2(\mathbf{tripy})_4]^{4+}$ with **2A-tripy**. However, even when $[Pd_2(\mathbf{tripy})_2(\mathbf{2A\text{-}tripy})_2]^{4+}$ was treated with 4 equiv of **2A-tripy**, there was no evidence for formation of the $[Pd_2(\mathbf{2A\text{-}tripy})_4]^{4+}$ cage (Figure 3h). Heating the solution of $[Pd_2(\mathbf{tripy})_2(\mathbf{2A\text{-}tripy})_2]^{4+}$ and **2A-tripy** (4 equiv) at 90 °C for 1 day led to no further substitution; the resulting ^{1}H NMR spectrum only displayed peaks due to the heteroleptic *cis*-$[Pd_2(\mathbf{tripy})_2(\mathbf{2A\text{-}tripy})_2]^{4+}$ cage and the two free ligands (**tripy** and **2A-tripy**). A solution of isolated *cis*-$[Pd_2(\mathbf{tripy})_2(\mathbf{2A\text{-}tripy})_2]^{4+}$ cage in d_6-DMSO was treated with 2 equiv of **2A-tripy** and left to stand at room temperature for 40 days (Supporting Information, Figure S1.14). Over this period there was negligible change observed in the ^{1}H NMR spectrum of *cis*-$[Pd_2(\mathbf{tripy})_2(\mathbf{2A\text{-}tripy})_2]^{4+}$, confirming the high metastability of the heteroleptic architecture (Supporting Information, Figure S1.14b). Heating an identical mixture at 50 °C led to decomposition and disappearance of cage ^{1}H NMR signals over a period of 7 days, rather than additional substitution (Supporting Information, Figure S1.14c). Interestingly, addition of 2 equiv of the **PEG-tripy**[28a] ligand to a solution of isolated *cis*-$[Pd_2(\mathbf{tripy})_2(\mathbf{2A\text{-}tripy})_2]^{4+}$ cage in d_6-DMSO at 298 K does lead to ligand displacement, and it is the **tripy** ligands that are liberated, not **2A-tripy**. Over a 10 day period, partial displacement of **tripy** occurred, giving an equilibrium mixture of roughly equal amounts of $[Pd_2(\mathbf{tripy})_2(\mathbf{2A\text{-}tripy})_2]^{4+}$, $[Pd_2(\mathbf{tripy})(\mathbf{PEG\text{-}tripy})(\mathbf{2A\text{-}tripy})_2]^{4+}$ and $[Pd_2(\mathbf{PEG\text{-}tripy})_2(\mathbf{2A\text{-}tripy})_2]^{4+}$ (Supporting Information, Figures S1.15 and S1.16). It was also established that treating $[Pd_2(\mathbf{tripy})_4]^{4+}$ with **PEG-tripy** did not lead to the same complete displacement of **tripy** as had been observed with **3A-tripy**, and instead generated randomly mixed heteroleptic cages that remained stable over a 10 day period (Supporting Information, Figures S1.17 and S1.18). We attribute this difference to the subtle weakening of ligand strength on going from the primary amine to the O-alkyl substituent in the 3-position of the terminal pyridines.

It seems that the preorganization of the $[Pd_2(\mathbf{tripy})_4]^{4+}$ cage architecture is important for the clean generation of the heteroleptic *cis*-$[Pd_2(\mathbf{tripy})_2(\mathbf{2A\text{-}tripy})_2]^{4+}$ system. Efforts to cleanly generate the heteroleptic cage by the direct combination of **tripy**, **2A-tripy**, and $[Pd(CH_3CN)_4](BF_4)_2$ in a 2:2:2 ratio were unsuccessful (Supporting Information, Figure S1.19 and S1.20). A mixture of heteroleptic products (including the mixed $[Pd_2(\mathbf{tripy})_2(\mathbf{2A\text{-}tripy})_2]^{4+}$ species) was obtained even after prolonged heating (90 °C) of the mixture. However, no homoleptic cages were detected in the ^{1}H NMR spectrum under these conditions (Supporting Information, Figure S1.19b).

Interestingly, combining $[Pd_2(\mathbf{tripy})_4]^{4+}$ and $[Pd_2(\mathbf{2A\text{-}tripy})_4]^{4+}$ in d_6-DMSO at 50 °C over a 10 day period resulted in an untidy ^{1}H NMR spectrum, indicative of the presence of various heteroleptic assemblies, together with slow disappearance of the peaks associated with the homoleptic assemblies, even though $[Pd_2(\mathbf{2A\text{-}tripy})_4]^{4+}$ is substantially lower in energy (Supporting Information, Figure S1.21). We attribute this interesting result to low levels of exchange with the coordinating solvent and thereby generated free ligands that would normally not be visible in an equilibrium highly favoring $[Pd_2(\mathbf{2A\text{-}tripy})_4]^{4+}$, in conjunction with a kinetic barrier preventing **2A-tripy** from re-associating with **2A-tripy**-containing $[Pd_2(\mathbf{L})_4]^{4+}$ assemblies.

In combination, the experimental and computational results suggest that the heteroleptic *cis*-$[Pd_2(\mathbf{tripy})_2(\mathbf{2A\text{-}tripy})_2]^{4+}$ is not the thermodynamic product of the reaction of $[Pd_2(\mathbf{tripy})_4]^{4+}$ with **2A-tripy**; rather, it is an extremely (meta)stable kinetic intermediate. Most commonly these types of pyridyl-ligated square planar palladium(II) complexes undergo associative ligand-exchange processes.[33] Our experimental evidence is consistent with a similar associative ligand-exchange processes occurring in these $[Pd_2(\mathbf{L}_{\mathbf{tripy}})_4]^{4+}$ systems. Despite **2A-tripy** being a stronger donor ligand[29] than **3A-tripy**, the ligand exchange is more rapid in the **3A-tripy** system. This suggests that the steric "bulk" of the **2A-tripy** ligand is hampering the formation of the five-coordinate intermediate/transition-state species and leads to a slower rate of reaction. Once *cis*-$[Pd_2(\mathbf{tripy})_2(\mathbf{2A\text{-}tripy})_2]^{4+}$ is formed, the addition of excess **2A-tripy** does not lead to further ligand displacement. However, addition of the less sterically hindered **PEG-tripy** does cause displacement of the **tripy** ligands from *cis*-$[Pd_2(\mathbf{tripy})_2(\mathbf{2A\text{-}tripy})_2]^{4+}$. The **2A-tripy** ligands are stronger donors than the **tripy** ligands,[29] and the *cis* orientation with the interligand hydrogen-bonding between the two **2A-tripy** ligands generates a *pseudo*-chelate system and makes them nonlabile. The **tripy** ligands of the *cis*-$[Pd_2(\mathbf{tripy})_2(\mathbf{2A\text{-}tripy})_2]^{4+}$ system remain labile and can be displaced by the **PEG-tripy** but not the **2A-tripy** ligands. Together, these results strongly suggest that there is a significant kinetic barrier to the addition of a third **2A-tripy** ligand to the cage assembly, which we believe is due to steric clashes and lone-pair repulsions between $[Pd_2(\mathbf{tripy})_2(\mathbf{2A\text{-}tripy})_2]^{4+}$ and the incoming **2A-tripy** ligand (Figure 6).[34]

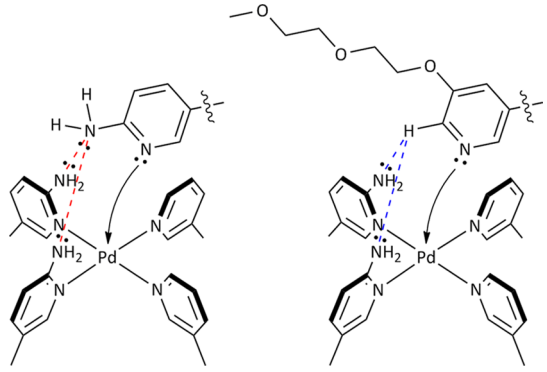

Figure 6. Pictorial representation of the increased steric and electronic barriers to additional substitution of **2A-tripy** to *cis*-$[Pd_2(\mathbf{tripy})_2(\mathbf{2A\text{-}tripy})_2]^{4+}$ (left) compared with **PEG-tripy** (right). Red dashed lines: lone pair−lone pair repulsions and steric clash. Blue dashed lines: hydrogen-bonding.

DOI: 10.1021/jacs.6b05629
J. Am. Chem. Soc. 2016, 138, 10578−10585

Thus, the 2-amino groups of the **2A-tripy** sterically shield the palladium(II) ions of the cage from incoming nucleophiles. Additionally, it is presumed that hydrogen-bonding interactions between the amino groups of the **2A-tripy** and acidic α-hydrogens of the adjacent **tripy** ligands also help to stabilize the mixed cage. These two effects combined make the mixed-ligand species relatively inert to further substitution with 2-substituted pyridyl ligands, while 3-substituted pyridyl donors can undergo further ligand exchange.

The observation that addition of **PEG-tripy** to $[Pd_2(\mathbf{tripy})_2(\mathbf{2A\text{-}tripy})_2]^{4+}$ generated an equilibrium mixture of roughly equal amounts of $[Pd_2(\mathbf{tripy})_2(\mathbf{2A\text{-}tripy})_2]^{4+}$, $[Pd_2(\mathbf{tripy})(\mathbf{PEG\text{-}tripy})(\mathbf{2A\text{-}tripy})_2]^{4+}$, and $[Pd_2(\mathbf{PEG\text{-}tripy})_4(\mathbf{2A\text{-}tripy})_2]^{4+}$ (*vide supra*) provided a potential experimental method for determining whether the *cis* or *trans* isomer of the heteroleptic $[Pd_2(\mathbf{L_a})_2(\mathbf{L_b})_2]^{4+}$ cages was present in solution (Figure 7). The formation of the heteroleptic triligand system

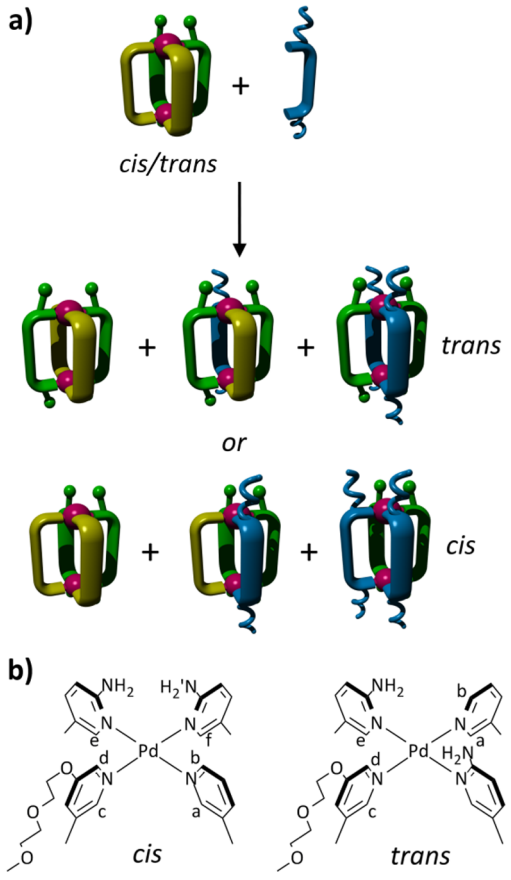

Figure 7. (a) Cartoon representation of the strategy employed to generate the equilibrium mixture containing $[Pd_2(\mathbf{tripy})(\mathbf{PEG\text{-}tripy})(\mathbf{2A\text{-}tripy})_2]^{4+}$, showing the products as they would exist in both the *cis* and *trans* forms. (b) Environments around the Pd(II) centers in the potential *cis* and *trans* isomers.

$[Pd_2(\mathbf{tripy})(\mathbf{PEG\text{-}tripy})(\mathbf{2A\text{-}tripy})_2]^{4+}$ generates *cis* and *trans* isomers with different symmetries that could be identified using ^{1}H NMR spectroscopy (Figure 7 and Supporting Information, Figures S1.22–S1.25).

The equilibrium mixture generated by adding the **PEG-tripy** ligands to a solution of isolated *cis*-$[Pd_2(\mathbf{tripy})_2(\mathbf{2A\text{-}tripy})_2]^{4+}$ cage in d_6-DMSO at 298 K displayed three sets of resonances that were attributable to palladium(II) cage species. Two of these species were readily identifiable as the mixed cages $[Pd_2(\mathbf{tripy})_2(\mathbf{2A\text{-}tripy})_2]^{4+}$ and $[Pd_2(\mathbf{PEG\text{-}tripy})_2(\mathbf{2A\text{-}tripy})_2]^{4+}$, which had been made independently (*vide infra*). The last downfield-shifted set of peaks, as might be expected, was the triple-ligand heteroleptic assembly $[Pd_2(\mathbf{tripy})(\mathbf{PEG\text{-}tripy})(\mathbf{2A\text{-}tripy})_2]^{4+}$. This species had a diffusion coefficient of 1.05×10^{-10} m^2 s^{-1}, consistent with the other cages, suggesting that it is another $[Pd_2(\mathbf{L_{tripy}})_4]^{4+}$ cage system. Mass spectral analysis of the reaction mixture showed ions consistent with the presence of the corresponding free ligands and the $[Pd_2(\mathbf{tripy})_2(\mathbf{2A\text{-}tripy})_2]^{4+}$ and $[Pd_2(\mathbf{PEG\text{-}tripy})_2(\mathbf{2A\text{-}tripy})_2]^{4+}$ heteroleptic cages. Additionally, the spectrum displayed a peak consistent with the $[Pd_2(\mathbf{tripy})(\mathbf{PEG\text{-}tripy})(\mathbf{2A\text{-}tripy})_2]^{4+}$ system (m/z = 431.0966, calcd = 431.0978, Supporting Information, Figure S1.16), confirming that the heteroleptic triligand cage was the third species observed in the ^{1}H NMR spectrum. Exploiting 2D COSY and ROESY ^{1}H NMR experiments, the proton resonances of the $[Pd_2(\mathbf{tripy})(\mathbf{PEG\text{-}tripy})(\mathbf{2A\text{-}tripy})_2]^{4+}$ cage could be fully assigned (Supporting Information, Figures S1.22–S1.25). The triligand species had two amino groups, identifiable through a 2D ROESY ^{1}H NMR coupling network as being part of the same structure, each of which in a different environment (NH_2 and NH_2' as labeled in Figure 7b), consistent with the *cis* isomer rather than the *trans*, which would possess only a single amino environment. These amino groups each exhibited 2D through-space coupling to two different protons (H_b and H_d), which in turn showed through-space coupling to each other, and hence are the two exohedral protons on **tripy** and **PEG-tripy**. In a similar fashion, coupling could be observed between the endohedral proton on **tripy** (H_a) and two other protons (H_c and H_f), again consistent with formation of the *cis* isomer. The NMR data provide strong indirect experimental evidence that the heteroleptic cages adopt the *cis* geometry, completely consistent with the calculated results.

Pleasingly, the method proved a general approach to heteroleptic $[Pd_2(\mathbf{L_a})_2(\mathbf{L_b})_2]^{4+}$ assemblies. Treatment of our previously reported *exo*-functionalized cages $[Pd_2(\mathbf{PEG\text{-}tripy})_4]^{4+}$ or $[Pd_2(\mathbf{Fc\text{-}tripy})_4]^{4+}$ (where **Fc-tripy**[35] contains a ferrocene 1,2,3-triazole group on the 4-position of the central pyridyl unit of the ligand) with 2.2 equiv of **2A-tripy** in d_6-DMSO resulted in the clean formation of the heteroleptic $[Pd_2(\mathbf{tripy\text{-}Fc})_2(\mathbf{2A\text{-}tripy})_2]^{4+}$ and $[Pd_2(\mathbf{PEG\text{-}tripy})_2(\mathbf{2A\text{-}tripy})_2]^{4+}$ cage assemblies (Supporting Information, Synthesis 1.9 and 1.10). Likewise, the $[Pd_2(\mathbf{dipy})_4]^{4+}$ cage[36] (where **dipy** = 1,3-bis(pyridin-3-ylethynyl)benzene ligand[37]) could be treated with 3 equiv of **2A-tripy** to give a $[Pd_2(\mathbf{dipy})_2(\mathbf{2A\text{-}tripy})_2]^{4+}$ assembly. The formation of the heteroleptic $[Pd_2(\mathbf{L_a})_2(\mathbf{L_b})_2]^{4+}$ architectures was again confirmed using a combination of ^{1}H, DOSY, and ROESY NMR spectroscopies and high-resolution ESI-MS (Supporting Information, Figures S1.26–S1.36 and Table S1.1).

As with the parent $[Pd_2(\mathbf{tripy})_2(\mathbf{2A\text{-}tripy})_2]^{4+}$ cage, the pure $[Pd_2(\mathbf{L_a})_2(\mathbf{L_b})_2]^{4+}$ assemblies could be isolated from the free ligands by exploiting solubility differences (Supporting Information, Synthesis 1.9). The chemical shifts for key resonances in the ^{1}H NMR spectra of these new heteroleptic assemblies are very similar to those observed in the parent $[Pd_2(\mathbf{tripy})_2(\mathbf{2A\text{-}tripy})_2]^{4+}$ cage, suggesting that the compounds all adopt the same *cis* geometry. These new cages display two different functional groups on the *exo* surfaces of the cage assemblies, suggesting that this method could provide a facile approach to lower symmetry, highly functionalized cage architectures.

DOI: 10.1021/jacs.6b05629
J. Am. Chem. Soc. 2016, 138, 10578–10585

CONCLUSION

The addition of electron-rich amino-substituted tripyridyl 2,6-bis(pyridin-3-ylethynyl)pyridine (**tripy**) ligands (with amino groups either in the 2- (**2A-tripy**) or 3-position (**3A-tripy**) of the terminal pyridines) to a preformed $[Pd_2(\mathbf{tripy})_4]^{4+}$ cage resulted in two different outcomes. Addition of the **3A-tripy** to the $[Pd_2(\mathbf{tripy})_4]^{4+}$ cage led to complete displacement of the **tripy** ligands and formation of the $[Pd_2(\mathbf{3A\text{-}tripy})_4]^{4+}$ system. More importantly, it was found that addition of free **2A-tripy** to a solution of the $[Pd_2(\mathbf{tripy})_4]^{4+}$ cage resulted in the clean generation of a heteroleptic $[Pd_2(\mathbf{tripy})_2(\mathbf{2A\text{-}tripy})_2]^{4+}$ architecture. The formation of the mixed-ligand cage was confirmed using ^{1}H, DOSY, and ROESY NMR spectroscopies and high-resolution ESI-MS. DFT calculations suggested the *cis* isomer is more stable than the *trans* isomer. They also indicated that the heteroleptic cage is not the thermodynamic product of the reaction of **2A-tripy** and $[Pd_2(\mathbf{tripy})_4]^{4+}$ but is rather a kinetically (meta)stable intermediate, and this was confirmed through additional exchange experiments. It is presumed that hydrogen-bonding interactions between the amino groups of the **2A-tripy** and acidic α-hydrogens of the adjacent **tripy** ligands help to stabilize the mixed cage. Additionally, the 2-amino groups of the **2A-tripy** sterically shield the palladium(II) ions of the cage from incoming nucleophiles. These two effects combined make the mixed-ligand species relatively inert to further substitution. Competition experiments showed that the heteroleptic $[Pd_2(\mathbf{tripy})_2(\mathbf{2A\text{-}tripy})_2]^{4+}$ architecture was stable in solution at room temperature for several months. During the competition experiments, the formation of a triple-ligand $[Pd_2(\mathbf{tripy})(\mathbf{PEG\text{-}tripy})(\mathbf{2A\text{-}tripy})_2]^{4+}$ cage architecture was observed. NMR experiments on this species confirmed that it was the *cis* isomer, providing strong experimental evidence that all the heteroleptic systems adopt the *cis* geometry. Finally, it was shown that the method was a general approach to heteroleptic palladium(II) cages. Three other systems, displaying different *exo* or *endo* functionality within the cages' assembly, were generated, suggesting that this method could be applied to the synthesis of a range of highly functionalized heteroleptic $[Pd_2(\mathbf{L}_{\mathbf{tripy}})_4]^{4+}$ cages. Presumably the system could be extended to include other species with a wide variety[25a,35a,38] of different *exo* or *endo* functionalities. These types of novel low-symmetry heteroleptic metallosupramolecular architectures may lead to interesting new biological,[11f] photophysical, and catalytic[39] properties.

ASSOCIATED CONTENT

Supporting Information

The Supporting Information is available free of charge on the ACS Publications website at DOI: 10.1021/jacs.6b05629.

Experimental details, ^{1}H, ^{13}C, and DOSY NMR and ESI-MS information, DFT calculations, and calculated structures (PDF)

Molecular models (TXT)

AUTHOR INFORMATION

Corresponding Author

*jcrowley@chemistry.otago.ac.nz

Notes

The authors declare no competing financial interest.

ACKNOWLEDGMENTS

The authors thank Dr. Dave McMorran for fruitful discussions. D.P. and J.E.B. thank the University of Otago for Ph.D. scholarships. K.C.G. thanks the MacDiarmid Institute for support. J.D.C. (Laurenson Award, LA307) and D.P. (MacQueen Summer Scholarship) thank the Otago Medical Research Fund for financial support.

REFERENCES

(1) For some selected recent reviews see: (a) Cook, T. R.; Stang, P. J. *Chem. Rev.* **2015**, *115* (15), 7001−7045. (b) Castilla, A. M.; Ramsay, W. J.; Nitschke, J. R. *Acc. Chem. Res.* **2014**, *47* (7), 2063−2073. (c) Smulders, M. M. J.; Riddell, I. A.; Browne, C.; Nitschke, J. R. *Chem. Soc. Rev.* **2013**, *42* (4), 1728−1754. (d) Young, N. J.; Hay, B. P. *Chem. Commun.* **2013**, *49* (14), 1354−1379. (e) Nakamura, T.; Ube, H.; Shionoya, M. *Chem. Lett.* **2013**, *42* (4), 328−334. (f) Beves, J. E.; Blight, B. A.; Campbell, C. J.; Leigh, D. A.; McBurney, R. T. *Angew. Chem., Int. Ed.* **2011**, *50* (40), 9260−9327. (g) Chakrabarty, R.; Mukherjee, P. S.; Stang, P. J. *Chem. Rev.* **2011**, *111* (11), 6810−6918. (h) Han, Y.-F.; Li, H.; Jin, G.-X. *Chem. Commun.* **2010**, *46* (37), 6879−6890. (i) Ward, M. D. *Chem. Commun.* **2009**, *30*, 4487−4499. (j) Glasson, C. R. K.; Lindoy, L. F.; Meehan, G. V. *Coord. Chem. Rev.* **2008**, *252* (8-9), 940−963.

(2) (a) Mal, P.; Breiner, B.; Rissanen, K.; Nitschke, J. R. *Science* **2009**, *324* (5935), 1697−1699. (b) Yamashina, M.; Sei, Y.; Akita, M.; Yoshizawa, M. *Nat. Commun.* **2014**, *5*, 4662−4668.

(3) (a) Peinador, C.; Pia, E.; Blanco, V.; Garcia, M. D.; Quintela, J. M. *Org. Lett.* **2010**, *12* (7), 1380−1383. (b) Blanco, V.; Garcia, M. D.; Terenzi, A.; Pia, E.; Fernandez-Mato, A.; Peinador, C.; Quintela, J. M. *Chem. - Eur. J.* **2010**, *16* (41), 12373−12380. (c) Riddell, I. A.; Smulders, M. M. J.; Clegg, J. K.; Nitschke, J. R. *Chem. Commun.* **2011**, *47* (1), 457−459.

(4) (a) Yoshizawa, M.; Fujita, M. *Bull. Chem. Soc. Jpn.* **2010**, *83* (6), 609−618. (b) Yoshizawa, M.; Klosterman, J. K.; Fujita, M. *Angew. Chem., Int. Ed.* **2009**, *48* (19), 3418−3438.

(5) (a) Brown, C. J.; Toste, F. D.; Bergman, R. G.; Raymond, K. N. *Chem. Rev.* **2015**, *115* (9), 3012−3035. (b) Leenders, S. H. A. M.; Gramage-Doria, R.; de Bruin, B.; Reek, J. N. H. *Chem. Soc. Rev.* **2015**, *44* (2), 433−448. (c) Lifschitz, A. M.; Rosen, M. S.; McGuirk, C. M.; Mirkin, C. A. *J. Am. Chem. Soc.* **2015**, *137* (23), 7252−7261. (d) Wiester, M. J.; Ulmann, P. A.; Mirkin, C. A. *Angew. Chem., Int. Ed.* **2011**, *50* (1), 114−137.

(6) (a) Therrien, B. *CrystEngComm* **2015**, *17* (3), 484−491. (b) Therrien, B. *Chem. - Eur. J.* **2013**, *19* (26), 8378−8386. (c) Therrien, B. *Top. Curr. Chem.* **2011**, *319*, 35−56.

(7) (a) Kaner, R. A.; Scott, P. *Future Med. Chem.* **2015**, *7* (1), 1−4. (b) Cook, T. R.; Vajpayee, V.; Lee, M. H.; Stang, P. J.; Chi, K.-W. *Acc. Chem. Res.* **2013**, *46* (11), 2464−2474.

(8) (a) Xu, L.; Wang, Y.-X.; Yang, H.-B. *Dalton Trans.* **2015**, *44* (3), 867−890. (b) Chepelin, O.; Ujma, J.; Wu, X.; Slawin, A. M. Z.; Pitak, M. B.; Coles, S. J.; Michel, J.; Jones, A. C.; Barran, P. E.; Lusby, P. J. *J. Am. Chem. Soc.* **2012**, *134* (47), 19334−19337.

(9) Croue, V.; Goeb, S.; Salle, M. *Chem. Commun.* **2015**, *51* (34), 7275−7289.

(10) (a) Li, H.; Yao, Z.-J.; Liu, D.; Jin, G.-X. *Coord. Chem. Rev.* **2015**, *293−294*, 139−157. (b) Saha, M. L.; Neogi, S.; Schmittel, M. *Dalton Trans.* **2014**, *43* (10), 3815−3834. (c) Saha, M. L.; De, S.; Pramanik, S.; Schmittel, M. *Chem. Soc. Rev.* **2013**, *42* (16), 6860−6909.

(11) (a) Wang, S.-Y.; Fu, J.-H.; Liang, Y.-P.; He, Y.-J.; Chen, Y.-S.; Chan, Y.-T. *J. Am. Chem. Soc.* **2016**, *138* (11), 3651−3654. (b) Metherell, A. J.; Ward, M. D. *Chem. Sci.* **2016**, *7* (2), 910−915. (c) Metherell, A. J.; Ward, M. D. *Chem. Commun.* **2014**, *50* (75), 10979−10982. (d) Ronson, T. K.; Roberts, D. A.; Black, S. P.; Nitschke, J. R. *J. Am. Chem. Soc.* **2015**, *137* (45), 14502−14512. (e) Yang, J.; Bhadbhade, M.; Donald, W. A.; Iranmanesh, H.; Moore, E. G.; Yan, H.; Beves, J. E. *Chem. Commun.* **2015**, *51* (21), 4465−4468. (f) Sato, S.; Ikemi, M.; Kikuchi, T.; Matsumura, S.; Shiba, K.; Fujita, M. *J. Am. Chem. Soc.* **2015**, *137* (40), 12890−12896.

DOI: 10.1021/jacs.6b05629
J. Am. Chem. Soc. 2016, 138, 10578−10585

(12) Ward, M. D.; Raithby, P. R. *Chem. Soc. Rev.* **2013**, *42* (4), 1619−1636.
(13) Debata, N. B.; Tripathy, D.; Chand, D. K. *Coord. Chem. Rev.* **2012**, *256* (17−18), 1831−1945.
(14) (a) Harris, K.; Fujita, D.; Fujita, M. *Chem. Commun.* **2013**, *49* (60), 6703−6712. (b) Han, M.; Engelhard, D. M.; Clever, G. H. *Chem. Soc. Rev.* **2014**, *43* (6), 1848−60.
(15) Fujita, M.; Tominaga, M.; Hori, A.; Therrien, B. *Acc. Chem. Res.* **2005**, *38*, 369−378.
(16) (a) Bar, A. K.; Raghothama, S.; Moon, D.; Mukherjee, P. S. *Chem. - Eur. J.* **2012**, *18* (11), 3199−3209. (b) Bar, A. K.; Mostafa, G.; Mukherjee, P. S. *Inorg. Chem.* **2010**, *49* (17), 7647−7649. (c) Ono, K.; Yoshizawa, M.; Kato, T.; Watanabe, K.; Fujita, M. *Angew. Chem., Int. Ed.* **2007**, *46* (11), 1803−1806. (d) Yoshizawa, M.; Ono, K.; Kumazawa, K.; Kato, T.; Fujita, M. *J. Am. Chem. Soc.* **2005**, *127* (31), 10800−10801.
(17) Approaches to heteroleptic metallosupramolecular architectures using more inert square planar platinum(II) complexes are more common. The organometallic molecular "clip" method (refs 17a−d) and the charge separation approach (refs 17e,f) both provide access to heteroleptic platinum(II)-based systems. For selected examples see: (a) Seidel, S. R.; Stang, P. J. *Acc. Chem. Res.* **2002**, *35* (11), 972−983. (b) Kuehl, C. J.; Yamamoto, T.; Seidel, S. R.; Stang, P. J. *Org. Lett.* **2002**, *4* (6), 913−915. (c) Kuehl, C. J.; Mayne, C. L.; Arif, A. M.; Stang, P. J. *Org. Lett.* **2000**, *2* (23), 3727−3729. (d) Wang, M.; Zheng, Y.-R.; Cook, T. R.; Stang, P. J. *Inorg. Chem.* **2011**, *50*, 6107−6113. (e) Wang, M.; Lan, W.-J.; Zheng, Y.-R.; Cook, T. R.; White, H. S.; Stang, P. J. *J. Am. Chem. Soc.* **2011**, *133* (28), 10752−10755. (f) Zheng, Y.-R.; Zhao, Z.; Wang, M.; Ghosh, K.; Pollock, J. B.; Cook, T. R.; Stang, P. J. *J. Am. Chem. Soc.* **2010**, *132* (47), 16873−16882.
(18) (a) Yamashina, M.; Yuki, T.; Sei, Y.; Akita, M.; Yoshizawa, M. *Chem. - Eur. J.* **2015**, *21* (11), 4200−4204. (b) Henkelis, J. J.; Fisher, J.; Warriner, S. L.; Hardie, M. J. *Chem. - Eur. J.* **2014**, *20* (14), 4117−4125.
(19) (a) Johnson, A. M.; Moshe, O.; Gamboa, A. S.; Langloss, B. W.; Limtiaco, J. F. K.; Larive, C. K.; Hooley, R. J. *Inorg. Chem.* **2011**, *50* (19), 9430−9442. (b) Johnson, A. M.; Hooley, R. J. *Inorg. Chem.* **2011**, *50* (11), 4671−4673.
(20) Kishi, N.; Li, Z.; Yoza, K.; Akita, M.; Yoshizawa, M. *J. Am. Chem. Soc.* **2011**, *133* (30), 11438−11441.
(21) Bhat, I. A.; Samanta, D.; Mukherjee, P. S. *J. Am. Chem. Soc.* **2015**, *137* (29), 9497−9502.
(22) Frank, M.; Krause, L.; Herbst-Irmer, R.; Stalke, D.; Clever, G. H. *Dalton Trans.* **2014**, *43* (11), 4587−4592.
(23) Sun, Q.-F.; Sato, S.; Fujita, M. *Angew. Chem., Int. Ed.* **2014**, *53* (49), 13510−13513.
(24) Howlader, P.; Das, P.; Zangrando, E.; Mukherjee, P. S. *J. Am. Chem. Soc.* **2016**, *138* (5), 1668−1676.
(25) (a) Elliott, A. B. S.; Lewis, J. E. M.; van der Salm, H.; McAdam, C. J.; Crowley, J. D.; Gordon, K. C. *Inorg. Chem.* **2016**, *55* (7), 3440−3447. (b) Kim, T. Y.; Lucas, N. T.; Crowley, J. D. *Supramol. Chem.* **2015**, *27* (11−12), 734−745. (c) Lewis, J. E. M.; Crowley, J. D. *Supramol. Chem.* **2014**, *26* (3−4), 173−181. (d) Lewis, J. E. M.; Crowley, J. D. *Aust. J. Chem.* **2013**, *66* (11), 1447−1454. (e) Crowley, J. D.; Steele, I. M.; Bosnich, B. *Inorg. Chem.* **2005**, *44* (9), 2989−2991. (f) Crowley, J. D.; Steele, I. M.; Bosnich, B. *Eur. J. Inorg. Chem.* **2005**, *2009* (19), 3907−3917. (g) Crowley, J. D.; Bosnich, B. *Eur. J. Inorg. Chem.* **2005**, *2005* (11), 2015−2025. (h) Crowley, J. D.; Bosnich, B. *Eur. J. Inorg. Chem.* **2005**, *2005* (11), 2015−2025. (i) Crowley, J. D.; Goshe, A. J.; Steele, I. M.; Bosnich, B. *Chem. - Eur. J.* **2004**, *10* (8), 1944−1955. (j) Crowley, J. D.; Goshe, A. J.; Bosnich, B. *Chem. Commun.* **2003**, *22*, 2824−2825.
(26) $[Pd_2(\mathbf{L})_4]$ cages are one of the most common types of metallosupramolecular architechiture. For selected examples see: (a) Ahmedova, A.; Momekova, D.; Yamashina, M.; Shestakova, P.; Momekov, G.; Akita, M.; Yoshizawa, M. *Chem. - Asian J.* **2016**, *11* (4), 474−477. (b) Zhukhovitskiy, A. V.; Zhong, M.; Keeler, E. G.; Michaelis, V. K.; Sun, J. E. P.; Hore, M. J. A.; Pochan, D. J.; Griffin, R. G.; Willard, A. P.; Johnson, J. A. *Nat. Chem.* **2016**, *8* (1), 33−41. (c) Zhu, R.; Luebben, J.; Dittrich, B.; Clever, G. H. *Angew. Chem., Int. Ed.* **2015**, *54* (9), 2796−2800. (d) Zhou, L.-P.; Sun, Q.-F. *Chem. Commun.* **2015**, *51* (94), 16767−16770. (e) Wei, S.-C.; Pan, M.; Fan, Y.-Z.; Liu, H.; Zhang, J.; Su, C.-Y. *Chem. - Eur. J.* **2015**, *21* (20), 7418−7427. (f) Han, M.; Michel, R.; He, B.; Chen, Y.-S.; Stalke, D.; John, M.; Clever, G. H. *Angew. Chem., Int. Ed.* **2013**, *52* (4), 1319−1323. (g) Mochizuki, M.; Inoue, T.; Yamanishi, K.; Koike, S.; Kondo, M.; Zhang, L.; Aoki, H. *Dalton Trans.* **2014**, *43* (48), 17924−17927. (h) Clever, G. H.; Kawamura, W.; Tashiro, S.; Shiro, M.; Shionoya, M. *Angew. Chem., Int. Ed.* **2012**, *51* (11), 2606−2609. (i) Desmarets, C.; Gontard, G.; Cooksy, A. L.; Rager, M. N.; Amouri, H. *Inorg. Chem.* **2014**, *53* (9), 4287−4294. (j) Desmarets, C.; Ducarre, T.; Rager, M. N.; Gontard, G.; Amouri, H. *Materials* **2014**, *7* (1), 287−301. (k) McMorran, D. A.; Steel, P. J. *Angew. Chem., Int. Ed.* **1998**, *37*, 3295−3297.
(27) Lewis, J. E. M.; Gavey, E. L.; Cameron, S. A.; Crowley, J. D. *Chem. Sci.* **2012**, *3* (3), 778−784.
(28) (a) Preston, D.; Fox-Charles, A.; Lo, W. K. C.; Crowley, J. D. *Chem. Commun.* **2015**, *51* (43), 9042−9045. (b) McNeill, S. M.; Preston, D.; Lewis, J. E. M.; Robert, A.; Knerr-Rupp, K.; Graham, D. O.; Wright, J. R.; Giles, G. I.; Crowley, J. D. *Dalton Trans.* **2015**, *44* (24), 11129−11136.
(29) Preston, D.; McNeill, S. M.; Lewis, J. E. M.; Giles, G. I.; Crowley, J. D. *Dalton Trans.* **2016**, *45* (19), 8050−60.
(30) For a schematic diagram showing all the competition experiments carried out during this work, see Supporting Information, Figure S1.1.
(31) We attempted to calculate the energies of the cages in a DMSO solvent field. Unfortunately, these optimizations did not converge on a minimum.
(32) An alternative computational approach was to use a homodesmotic reaction ($[Pd_2(\mathbf{tripy})_4]^{4+}$ + $[Pd_2(\mathbf{2A\text{-}tripy})_4]^{4+}$ → $2[Pd_2(\mathbf{tripy})_2(\mathbf{2A\text{-}tripy})_2]^{4+}$ (either *cis* or *trans*)) to obtain the relative energies for the formation for the *cis* and *trans* isomers. The results are presented in the Supporting Information and are consistent with the values we derived using Hess's law. Both the *cis*- and *trans*-$[Pd_2(\mathbf{tripy})_2(\mathbf{2A\text{-}tripy})_2]^{4+}$ (*cis*, 48.8 kJ mol^{-1}; *trans*, 103.3 kJ mol^{-1}) are energetically uphill from the homoleptic cages, consistent with them not being the thermodynamic product of the reaction. The *cis* isomer is again found to be lower in energy that the *trans* (−27.2 kJ mol^{-1}), consistent with the *cis* isomer being more stable due to the hydrogen-bonding interaction between the 2-amino groups of the **2A-tripy** ligands.
(33) (a) Lo, W. K. C.; Cavigliasso, G.; Stranger, R.; Crowley, J. D.; Blackman, A. G. *Inorg. Chem.* **2014**, *53* (7), 3595−3605. (b) Hiraoka, S. *Chem. Rec.* **2015**, *15* (6), 1144−1147. (c) Tsujimoto, Y.; Kojima, T.; Hiraoka, S. *Chem. Sci.* **2014**, *5* (11), 4167−4172.
(34) While the incoming **Ltripy** nucleophiles can theoretically attack from either the *exo* or *endo* face of the $[Pd(py)_4]^{2+}$ planes, *endo* attack is extemely unlikely due to the steric protection provided by the ligand backbones.
(35) (a) Lewis, J. E. M.; Elliott, A. B. S.; McAdam, C. J.; Gordon, K. C.; Crowley, J. D. *Chem. Sci.* **2014**, *5* (5), 1833−1843. (b) Lewis, J. E. M.; McAdam, C. J.; Gardiner, M. G.; Crowley, J. D. *Chem. Commun.* **2013**, *49* (33), 3398−3400.
(36) Liao, P.; Langloss, B. W.; Johnson, A. M.; Knudsen, E. R.; Tham, F. S.; Julian, R. R.; Hooley, R. J. *Chem. Commun.* **2010**, *46* (27), 4932−4934.
(37) Kilpin, K. J.; Gower, M. L.; Telfer, S. G.; Jameson, G. B.; Crowley, J. D. *Inorg. Chem.* **2011**, *50* (3), 1123−1134.
(38) Lewis, J. E. M.; McAdam, C. J.; Gardiner, M. G.; Crowley, J. D. *Chem. Commun.* **2013**, *49* (33), 3398−3400.
(39) (a) Wang, Q.-Q.; Gonell, S.; Leenders, S. H. A. M.; Duerr, M.; Ivanovic-Burmazovic, I.; Reek, J. N. H. *Nat. Chem.* **2016**, *8* (3), 225−230. (b) Leenders, S. H. A. M.; Dürr, M.; Ivanović-Burmazović, I.; Reek, J. N. H. *Adv. Synth. Catal.* **2016**, *358* (9), 1509−1518. (c) Gramage-Doria, R.; Hessels, J.; Leenders, S. H. A. M.; Troeppner, O.; Duerr, M.; Ivanovic-Burmazovic, I.; Reek, J. N. H. *Angew. Chem., Int. Ed.* **2014**, *53* (49), 13380−13384.

DOI: 10.1021/jacs.6b05629
J. Am. Chem. Soc. 2016, 138, 10578−10585